

# Vision System: Image and Wear Analysis Using Machine Vision

Zhang Hainan\*

Department of Otolaryngology-Head and Neck Surgery, Saint Louis University School of Medicine, Saint Louis, MO, USA

## Abstract

Monitoring tool wear is extremely necessary in machining business because it could lead to loss of dimensional accuracy and quality of finished product. This work includes the event of machine vision system for the direct mensuration of flank wear of inorganic compound cutter inserts. This method consists of a camera to capture the tool wear image, a decent source of illumination to illuminate the tool, and a pc for image process. A brand new approach of inline automatic standardization of an element is planned during this work. The captured pictures of inorganic compound insert square measure processed, and therefore the segmental tool wear zone has been obtained by image process. The vision system extracts tool wear parameters like average tool wear dimension, tool wear space, and gear wear perimeter. The results of the common tool wear dimension obtained from the vision system square measure by experimentation valid with those obtained from the digital magnifier. A mean error of three was found for measurements of all twelve inorganic compound inserts. Scanning negatron micrographs of the wear and zone indicate the severe abrasion marks and damage to the innovative for higher machining time. This study indicates that the economical and reliable vision system is developed to live the tool wear parameters.

## Introduction

Measurement of tool wear is extraordinarily necessary to predict the helpful lifetime of tool inserts. This can be useful to watch and to check the results of the tool decline quality of machined work and economy of producing method. There square measure 2 main ways to live tool wear: indirect and direct ways. Within the indirect technique, tool wear is calculable with the signals coming back from differing types of sensors like surface texture of machined work, acoustics, vibration, feed forces, and current consumption. The tool wear prediction model is ready supported the magnitude of collected signals. Different technique for the mensuration of tool wear is that the direct mensuration over the tool wear zone [1]. There square measure 2 main tool wear types: flank wear and crater wear. The flank wear is wide wont to quantify the severity of tool wear. Characteristics of qualitative and quantitative morphology of tool wear square measure of nice concern for researchers these days. A lot of morphological options apart from normally thought-about parameter, i.e., average tool wear dimension, square measure needed for higher analysis of the particular condition of tool which might have an effect on machining method and quality of machined workpieces. The study shows that there's distinguished result of those new tool wear parameters on manufacturing quality workpieces associated conjointly has an economic advantage by creating ways for timely dynamic tool inserts. Tool wear usually ends up in loss in dimensional accuracy of finished product, potential injury to work, and reduce in surface integrity and amplification of chatter. Elaborated review for the tool condition observation indicates that the machine vision system is extraordinarily helpful for the direct mensuration of assorted forms of tool wear. Some applied mathematics approaches also are helpful in conjunction with machine vision system to search out tool wear [2]. Some researchers developed their own rule for the sting detection and segmentation of tool zone. White light-weight interferometry and stereo vision technique square measure used for the mensuration of volumetrically wear in crater in addition as flank wear region [3].

Various ways square measure prompt for the web and offline condition observation of the machining tool. Danesh and Khalili measured tool wear in terms of surface texture of the work throughout the turning method mistreatment undecimated ripple rework and applied mathematics options of the surface irregularities [4]. Yu et al. used morphological element analysis and edge observation

techniques to detect the damage edges beneath carrying operating conditions. D'Addona and Teti used artificial neural network for the automated and period analysis of the crater wear depth throughout quasiorthogonal cutting tests on AISI 1045 steel mistreatment wolfram inorganic compound insert [5]. Xiong et al. developed a picture process rule mistreatment Matlab to live the tool wear space. The image acquisition system consists of high resolution CCD camera, fluorescent high-frequency linear lights, and knowledge acquisition module. Schmitt et al. developed associate automatic tool wear observation system supported the active contour rule and neural networks for the flank wear mensuration. Fernandez-Robles et al. developed associate rule to live the defects in cutting edges of edge inserts on-line while not distressing the machining operation. A three-stage rule consists of edge conserving smoothing filter, computation of image gradient, and assessment of harm of innovative mistreatment geometrical properties [6].

Current work is targeted on the mensuration of flank wear mistreatment the machine vision system. a brand new approach of inline automatic standardization is planned here. Average tool wear dimension, tool wear space, and gear wear perimeter square measure measured mistreatment the machine vision system of these tool wear parameters square measure related with the machining time.

## Methodology

A schematic diagram of the tool wear mensuration system is shown in (Figure 1). The camera was used for capturing the image of done in tool inserts. Junction rectifier was used for illumination purpose

\*Corresponding author: Zhang Hainan, Department of Otolaryngology-Head and Neck Surgery, Saint Louis University School of Medicine, Saint Louis, MO, USA, E-mail: Hainanzhang456@edu.org

Received: 02-Nov-2022, Manuscript No: omoa-22-82420, Editor assigned: 04-Nov-2022, PreQC No: omoa-22-82420 (PQ), Reviewed: 18-Nov-2022, QC No: omoa-22-82420, Revised: 24-Nov-2022, Manuscript No: omoa-22-82420 (R), Published: 30-Nov-2022, DOI: 10.4172/2476-2075.1000178

Citation: Hainan Z (2022) Vision System: Image and Wear Analysis Using Machine Vision. Optom Open Access 7: 178.

Copyright: © 2022 Hainan Z. This is an open-access article distributed under the terms of the Creative Commons Attribution License, which permits unrestricted use, distribution, and reproduction in any medium, provided the original author and source are credited.

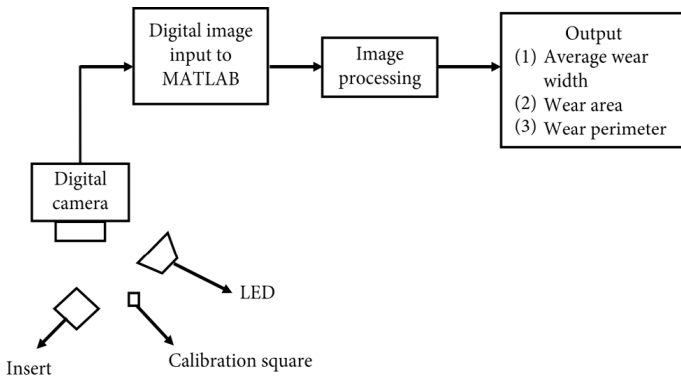
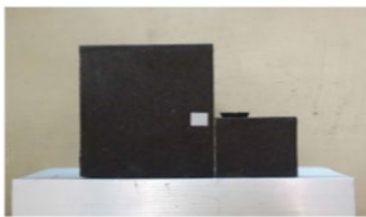


Figure 1: Schematic diagram of the tool wear measurement system.



(a)



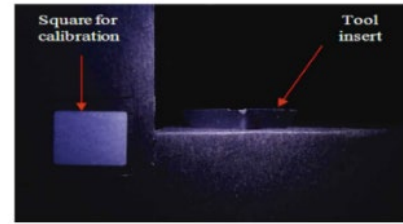
(b)

Figure 2: (a) Fixture for positioning of the tool insert and calibration square; (b) set up for the vision system.

of tool insert and standardization sq. The fixture has been developed for correct positioning of tool insert and therefore the standardization sq. (Figure 2a) shows the designed fixture for this purpose [7]. The standardization sq. was affixed on a vertical plate of fixture. The fixture was lined with a black paper to avoid the reflection of sunshine. This sq. is additionally used for outlining the origin of the virtual system developed for the mensuration of tool wear volume. The vertical plate has provision to maneuver forward and backward in order that the plane of standardization sq. and tip of tool insert remains same. The position of the camera, source of illumination, fixture, and insert is indicated in (Figure 2b). The image has been captured specified it contains each the standardization sq. and gear insert as indicated in (Figure 3a). (Figure 3b) shows the processed image of the standardization sq. [8]. (Figure 4) shows a flow diagram of associate rule for image process to calculate tool wear parameters (Figure 5) indicates the results of various stages of the image processing algorithm. (Figure 5a) indicates the grayscale image of the tool wear zone. (Figure 5b) indicates the binary image of the segmented tool wear zone obtained by using Otsu’s thresholding method [9].

**Results**

In this section, the ultimate results of measurements of 3 tool wear



(a)

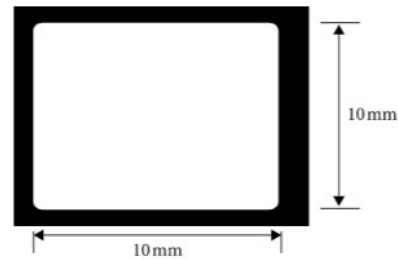


Figure 3: (a) Captured image of the worn out insert; (b) processed image of the calibration square.

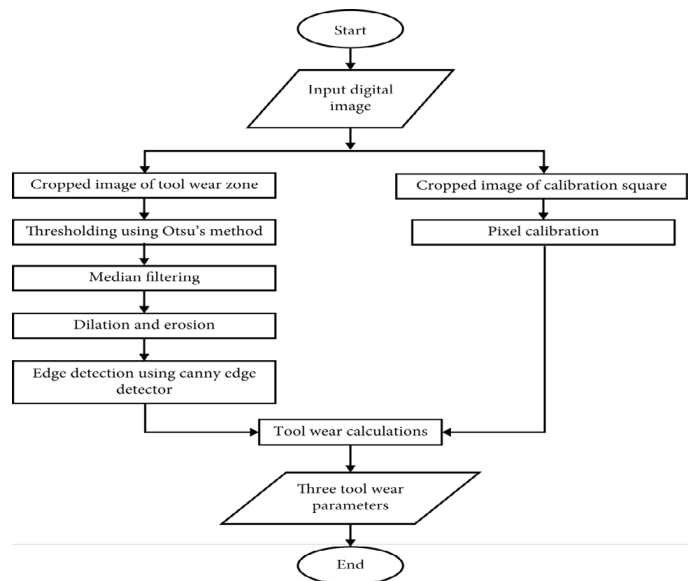
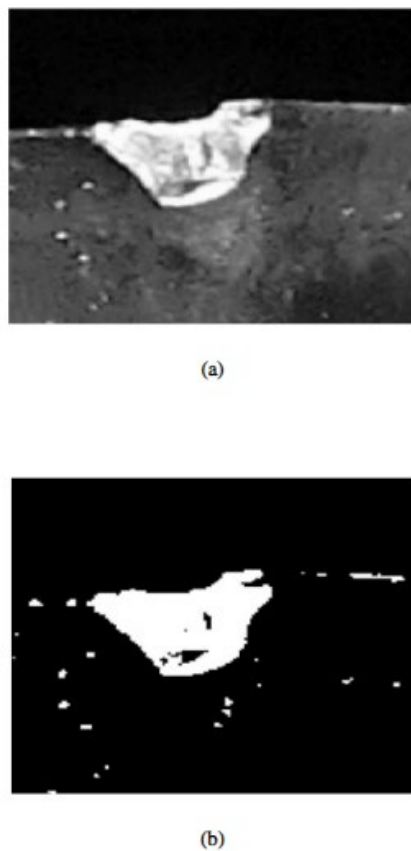


Figure 4: Flowchart of the algorithm for image processing.

parameters measured by the vision system are given. For the measuring of the damage of tool insert, the turning experiments area unit conducted on low steel that is wide used for the assembly of bearing cowl of AN IC engine. Turning operations area unit conducted on a CNC turning machine for the machining of internal diameter [10].

The details of the machining parameters area unit indicated in (Table 1). For each turning operation, contemporary inorganic compound insert was employed in that the machining and machining parameters were unbroken same. Machining time needed for each specimen was around five minutes [11]. (Table 2) indicates the small print of machining times for all the inserts. When the machining operation, the tool wear parameters of all the inserts were measured by the vision system [12]. So as to validate the accuracy of the developed



**Figure 5:** Results of various stages of the image processing algorithm indicating (a) actual grayscale image and images (b) obtained after thresholding, filtering, dilation, erosion, and edge detection, respectively.

**Table 1:** Details of the machining parameters.

Workpiece outer diameter	240 mm
Workpiece inside diameter	97 mm
Spindle speed	300 rpm
Feed rate	0.3 mm/revolution
Depth of cut	2 mm
Machining duration	5 minutes

**Table 2:** Machining time of all carbide inserts.

Insert number	1	2	3	4	5	6	7	8	9	10	11	12
Number of workpieces machined	1	2	3	4	5	6	7	8	9	10	11	12
Machining time (min)	5	10	15	20	25	30	35	40	45	50	55	60

**Table 3:** Measured parameters of the tool wear with the vision system.

Insert number	Average tool wear width (mm)	Tool wear area (mm <sup>2</sup> )	Tool wear perimeter (mm)
1	5	—	—
2	10	0.169	0.160
3	15	0.108	0.126
4	20	0.155	0.170
5	25	0.183	0.178
6	30	0.206	0.198
7	35	0.208	0.194
8	40	0.278	0.322
9	45	0.286	0.327
10	50	0.290	0.331
11	55	0.460	0.589
12	60	0.506	0.644

system, the common tool wear dimension for all inserts was conjointly measured employing a digital magnifier. (Table 3) indicates the pictures of the damage zones of all the inorganic compound inserts. These pictures area unit obtained when the process of actual pictures of tool wear by the machine vision system. These pictures area unit wont to mechanically verify the damage dimension of the inorganic compound inserts. Wear dimension is measured at 5 locations, and therefore the average price of the damage dimension is set and compared with the readings of the digital magnifier [13]. The magnitudes of average wear dimension obtained by the vision system and therefore the digital magnifier area unit fairly shut for all the inserts. A median error of roughly third-dimensional between each the readings indicates that the machine vision system will properly estimate the magnitude of tool wear. (Figure 6) indicates the comparison of the common wear dimension obtained by each the techniques. Tool wear dimension is seen increasing with the machining time in nearly linear fashion. Once the insert is employed for the machining of multiple workpieces, it undergoes the abrasion marks because of friction between the work surface and therefore the innovative. And it will increase with the amount of machined workpieces or machining time [14].

### Conclusion

The inline automatic activity system was with success enforced

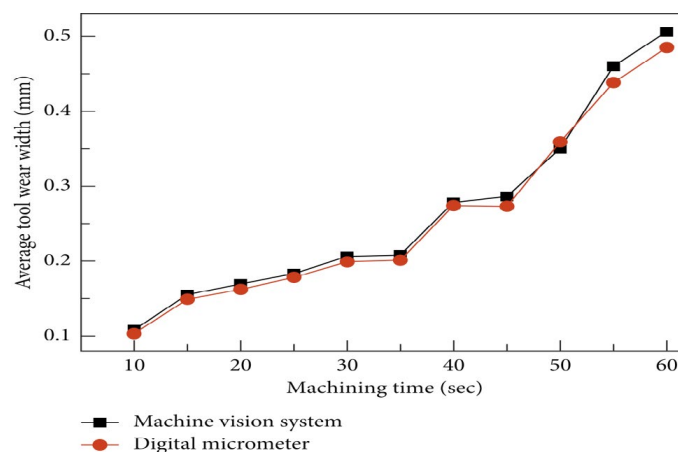


**Figure 6:** Graph comparing the digital microscope and the vision system measurements of average tool wear width.

for the measuring of tool wear parameters. With this activity system, there's no would like for separate activity of the vision system. The measurements of a median tool wear dimension with this vision system area unit found to be in shut agreement therewith with the digital magnifier. The common absolute error in mensuration average tool wear dimension for all the twelve inserts was found to be three.08%. Average wear dimension, wear area, and wear perimeter were seen increasing with the machining time. The scanning negatron micrographs indicate severe abrasion marks and harm to the innovative within the case of upper machining time. This study shows that the machine vision system will be effectively wont to live all tool wear parameters and therefore presents the proper and complete image of the tool wear. This system is going to be extraordinarily helpful for producing business to observe tool wear effectively instead of relying just one parameter. This may be extraordinarily helpful to review the results of tool decline quality of machined surface and economy of machining method.

### Conflicts of Interest

The authors declare that there are no conflicts of interest regarding the publication of this paper.

### References

1. Ames A (1935) Aniseikonia-a factor in the functioning of vision. *Am J Ophthalmol* 18: 1014-1020.
2. Rutstein RP, Corliss DA, Fullard RJ (2000) Comparison of aniseikonia as measured by the aniseikonia inspector and the space eikonometer. *Optom Vis Sci* 83: 836-842.
3. Langenbucher AS (2008) Anisometropia and aniseikonia-unsolved problems of cataract surgery. *Klin Monbl Augenheilkd* 225: 763-769.
4. Okamoto F, Sugiura Y, Okamoto Y (2012) Associations between metamorphopsia and foveal microstructure in patients with epiretinal membrane. *Invest Ophthalmol Vis Sci* 53: 6770-6775.
5. Okamoto F, Sugiura Y, Okamoto Y (2014) Time course of changes in aniseikonia and foveal microstructure after vitrectomy for epiretinal membrane. *Ophthalmol* 121: 2255-2260.
6. Kim JH, Kang SW, Kong MG (2013) Assessment of retinal layers and visual rehabilitation after epiretinal membrane removal. *Graefes Arch Clin Exp Ophthalmol* 251: 1055-1064.
7. Benegas NM, Egbert J, Engel WK (1999) Diplopia secondary to aniseikonia associated with macular disease. *Arch Ophthalmol* 117: 896-899.
8. Enoch JM (1997) Management of aniseikonia after intraocular lens implantation or refractive surgery. *J Refract Surg* 13: 79-82.
9. Okamoto F, Sugiura Y, Okamoto Y (2017) Aniseikonia in various retinal disorders. *Graefes Arch Clin Exp Ophthalmol* 255: 1063-1071.
10. Rutstein RP, Fullard RJ, Wilson JA (2015) Aniseikonia induced by cataract surgery and its effect on binocular vision. *Optom Vis Sci*. 92: 201-207.
11. Hodgetts D (2012) Nonsurgical management of diplopia after retinal surgery. *Am Orthopt J* 62: 38-43.
12. Renne G, Benson J, Charnwood L (1953) The physiological basis of sensory fusion. *Acta Ophthalmol* 34: 1-26.
13. Bradley A, Rabin J, Freeman RD (1983) Nonoptical determinants of aniseikonia. *Invest Ophthalmol Vis Sci*. 24: 507-512.
14. De Wit GC, Muraki CS (2006) Field-dependent aniseikonia associated with an epiretinal membrane a case study. *Ophthalmol* 113: 58-62.